

## 5.5 Analysis of Thermal Properties

The loose surface material of active dunes heats up very quickly and cools rapidly at night. The consolidated surfaces of inactive dunes retain the heat after sunset [*Fenton and Mellon, 2006*]. Thus, significant information on the capability of sand to be transported by wind can be derived from an analysis of the thermal properties of dune surfaces. Night-time brightness temperatures, i.e. an analysis of dune surface temperatures at night, can provide useful information about the material's condition. Furthermore, thermal inertia forms a reliable basis for estimating the average grain size of a particulate surface material, thus indicating whether or not a dune is movable. Therefore, the results of the following analyses will be used to assess the mobility of the dark deposits. This can only be done by a combined interpretation of all values measured, which will be presented in Sect. 5.6.

### 5.5.1 Optical and Thermal Thickness

Before interpreting the values obtained it is necessary to consider that the material composing the surface under analysis is *optically and thermally thick*. This ensures that the observed visible and thermal properties belong to the material deposited on the surface and not to the underlying bedrock. *Optically thin* materials have no influence on observed visible properties (less than  $\sim 1 \mu\text{m}$ ). For an *optically intermediate* deposit, the visible properties observed are a combination of the surface deposit's properties and the properties of the underlying material. *Optically thick* deposits are the only medium that determines the visible properties of the surface, such as its albedo. However, not very much material is needed to cause an albedo change and thus to be optically visible. The exact figure depends on several physical properties, such as composition, grain size, grain shape, packing, etc., but in general the deposit must be thicker than a few microns (e.g. must exceed the observation wavelength) [*Pelkey et al., 2001*]. *Edgett and Christensen* (1994), for example, estimated the optical thickness of a dust cover of some inter-dune areas in Oxia Palus to be around tens of micrometers.

To affect the surface temperature, a deposit must be *thermally thick*. A thermally thick deposit must be at least one diurnal skin depth thick. *Jakosky et al.* (1986) defined the diurnal thermal skin depth for a simple homogeneous surface as

$$\delta = \left( \frac{\kappa}{\rho c} * \frac{p}{\pi} \right)^{1/2} \quad (5)$$

where  $p$  is the length of a day,  $\kappa$  is thermal conductivity,  $\rho$  is bulk density, and  $c$  is specific heat [*Jakosky*, 1986; *Pelkey et al.*, 2001]. One diurnal skin depth for medium sand on Mars is about 7.5 cm [*Edgett and Christensen*, 1991; *Ferguson et al.*, 2006b] while for air fall dust it is about 1 cm [*Pelkey et al.*, 2001]. *Thermally intermediate* or *thermally thin* deposits influence the surface temperature only partially or not at all, respectively.

To conclude, thermal inertia values may only be interpreted as indicating absolute particle size when the observed material is both particulate and thermally thick [*Pelkey et al.*, 2001].

In this study, thermal sand sheet thickness was not calculated. However, if a sand sheet on a crater floor did not show a thermal signal distinct from that of the crater floor it was categorised as thermally thin. Finally, for these localities, thermal information was not used to identify the material condition.

### 5.5.2 Surface Brightness Temperature

Surface brightness temperature is derived from THEMIS night-time infrared data that provide brightness temperature records (BTRs) of the surfaces observed (cf. Sect. 4.3). On that basis, the relative temperature differences between the dunes and the crater floors could be determined. Dunes consisting of loose sand-sized material should be cooler than the surrounding crater floor. Conversely, consolidated dunes may show higher night-time temperatures than their surroundings. This THEMIS differential BTR analysis provides an impression of the night-time thermal behaviour of the dunes and sand sheets at the adequate spatial resolution of 100 m. These results are needed in evaluating TES TI data, which do not provide a satisfactory resolution of the dunes anyway. Moreover, the influence of a possible dust cover may be demonstrated by the differential BTR analysis in addition to the differential albedo examination, which reveals the optical thickness of dust on a surface (Sect. 5.5.1). If a dust cover is thermally thick, it will decrease the surface temperatures of both a dune and its surroundings and might mask the temperature difference noticeably. In localities where a dust influence had to be expected, the presence or absence of a dust cover was checked by a spectral analysis of the dune surfaces and the surrounding areas. The interpretation for the locality concerned was done very carefully.

There are dunes with significantly higher temperatures at night as well as dunes showing significantly lower temperatures at night in comparison to their surroundings.

Additionally, there are some dark deposits, which show no considerable temperature difference to the crater floor. Fig. 54 provides examples of the first two cases. The dune field in Fig. 54a shows lower night-time temperatures relative to its surrounding indicating that it might consists of loose material. The dune field in Fig. 54b consists of material that keeps heat at night unlike loose material and thus indicates that the dunes in this crater might have undergone a certain induration process.

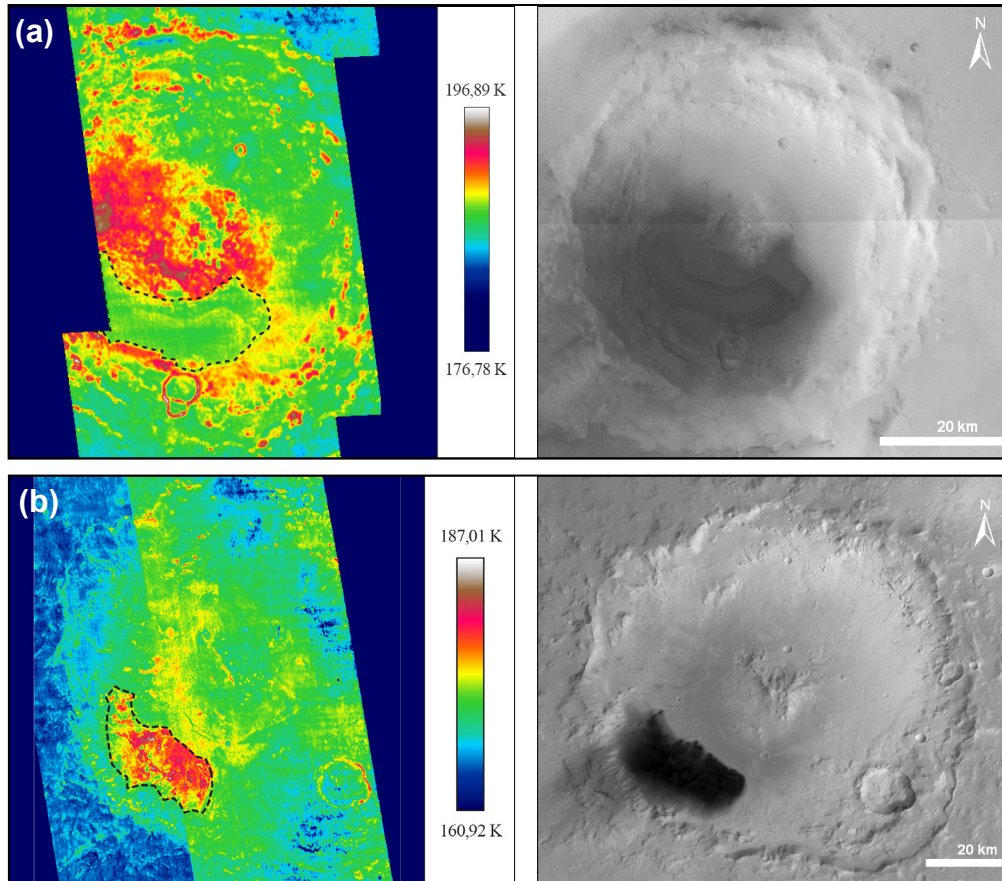


**Figure 54:** THEMIS brightness temperature analysis of dune fields. The mosaics show normalised surface temperatures. Dune fields are outlined by black dotted lines.

**(a)** Left: Night-time cold dune field relative to its surroundings in a crater in Elysium Planitia (9.6°N, 105.1°E). The mean absolute temperature of the dune field is about 185 K (measured from I06168009). Right: Corresponding HRSC nadir image (0032\_0000). **(b)** Left: Night-time warm dune field relative to its surroundings in Peridier Crater (25.8°N, 83.9°E). The mean absolute temperature of the dune field is about 190–195 K (measured from I06707051). Right: Corresponding HRSC nadir image (1530\_0000).

BTRs make sense in this context only if temperature differentials between dark deposits and their surroundings are compared. Comparing individual absolute temperatures cannot provide useful information, the reason being that environmental temperatures at the individual localities differ due to distinct regional climatic conditions, which depend on elevation and latitude. Thus, absolute brightness temperature values of dark deposits cannot be compared in a global context because they mostly reflect properties of the locality, not of the dark deposit.

### 5.5.3 Thermal Inertia

While the brightness temperature can only provide qualitative suggestions, thermal inertia provides reliable information about a material's physical surface condition. It is a measure of a material's thermal response to the diurnal heating cycle, expressing its resistance to temperature changes. As demonstrated in Sect. 4.4, thermal inertia is closely related to properties such as particle size, degree of induration, abundance of rocks, and exposure of bedrocks [Edgett and Christensen, 1991; Mellon *et al.*, 2000; Pelkey *et al.*, 2001]. Early investigations of thermo physical properties of dark intra-crater material were done by Christensen (1983) revealing a thermal inertia difference between the dark polar deposits and the crater material, as well as higher thermal values of the intra-crater deposits in comparison to the surrounding in many places.

Thermal inertia values for every crater were derived from TES data (Sect. 4.4). This information indicating grain size was used to judge which dunes are unconsolidated and therefore active and which are covered by an indurated surface and therefore inactive. In general, unconsolidated fines (i.e. dust, fine sand) will have low thermal inertia values, sand-sized particles intermediate TIs, and rocks, duricrusts, and exposed bedrock will have high TI values. On that basis, those dunes that show low or intermediate TI values are supposed to be active, while dunes showing higher TI values corresponding to duricrust are supposed to be consolidated. TI values may be converted into to effective grain sizes by an equation developed by Presley and Christensen (1997b). It is derived from laboratory studies and describes the relationship between thermal conductivity and particle diameter

$$\kappa = (CP^{0.6})d^{(-0.11\log P/K)} \quad (6)$$

where  $\kappa$  is thermal conductivity,  $P$  is atmospheric pressure,  $d$  is the particle diameter (in  $\mu\text{m}$ ), and  $C$  and  $K$  are constants with  $C \approx 0.0015$ , and  $K \approx 8.1 \times 10^4 \text{ torr}$  if units of  $\text{W/m K}$  are used for thermal conductivity and torr is used for pressure [Presley and Christensen, 1997b; Presley, 2002]. This  $\kappa$  value can then be inserted into the thermal inertia equation (3) from which the particle diameter can be resolved (using an average Martian surface pressure, e.g. 6 torr [Presley and Christensen, 1997b], and assuming  $\rho c$  to be  $1 \times 10^6 \text{ J m}^{-3} \text{ K}$ , which is valid for most geologic materials [Neugebauer *et al.*, 1971; Pelkey *et al.*, 2001; Presley, 2002; Ferguson *et al.*, 2006a]). However, this equation is only valid for particle sizes ranging from  $<10 \mu\text{m}$  to  $900 \mu\text{m}$  or thermal inertia values below  $350 \text{ J m}^{-2} \text{ K}^{-1} \text{ s}^{-1/2}$  [Presley and Christensen, 1997b; Pelkey *et al.*, 2001].

In order to apply a uniform classification to the whole range of TI value derived in this study, the classification of TI values and corresponding particle sizes for silicate minerals by Edgett and Christensen (1994) adapted from Fig. 2 in Edgett and Christensen (1991) are used (Table 10). These calculations are based on the nominal dependence of particle size on thermal inertia and thermal conductivity, and assume an average surface pressure of 6.5 mbar [Kieffer *et al.*, 1973; Edgett and Christensen, 1991]. Note that these values are in turn adapted from calculations made by Kieffer *et al.* (1973) who used data

from *Wechsler and Glaser* (1965). Calculations of the grain size of Martian surface materials derived from thermal inertia have been made by many authors [e.g. *Jakosky*, 1986; *Edgett and Christensen*, 1994; *Christensen et al.*, 1998; *Jakosky et al.*, 2000; *Christensen et al.*, 2001; *Pelkey et al.*, 2001; *Ferguson and Christensen*, 2003; *Fenton and Mellon*, 2006].

**Table 10:** Thermal inertia values and corresponding particle sizes  
(adapted from [*Edgett and Christensen*, 1994]).

<i>Wentworth (1922)</i> Classification		Grain Size Range, $\mu\text{m}$	
Clay (clay)		0 - 3.9	
Silt (silt)		3.9 - 62.5	
Very fine sand (vfs)		62.5 - 125	
Fine sand (fs)		125 - 250	
Medium sand (ms)		250 - 500	
Coarse sand (cs)		500 - 1000	
Very coarse sand (vcs)		1000 - 2000	
Granules (g)		2000 - 4000	
Pebbles (p)		4000 - 64,000	
Thermal Inertia $\text{Jm}^{-2} \text{s}^{-1/2} \text{K}^{-1}$	Thermal Inertia $10^{-3} \text{cal cm}^{-2} \text{s}^{-1/2} \text{K}^{-1}$	Grain size, * $\mu\text{m}$	Classification
80	1.9	$30 \pm 15$	silt
100	2.4	$40 \pm 15$	silt
120	2.9	$60 \pm 20$	silt-vfs
140	3.3	$70 \pm 20$	silt-vfs
160	3.8	$90 \pm 30$	vfs
180	4.3	$120 \pm 30$	vfs-fs
200	4.8	$140 \pm 40$	vfs-fs
220	5.3	$180 \pm 50$	fs
240	5.7	$210 \pm 60$	fs-ms
260	6.2	$260 \pm 60$	fs-ms
280	6.7	$310 \pm 60$	ms
300	7.2	$370 \pm 70$	ms
320	7.6	$400 \pm 80$	ms
340	8.1	$500 \pm 100$	ms-cs
360	8.6	$580 \pm 120$	ms-cs
380	9.1	$710 \pm 150$	cs
400	9.6	$800 \pm 200$	cs
420	10.0	$900 \pm 220$	cs-vcs
440	10.5	$1000 \pm 300$	cs-vcs
460	11.0	$1100 \pm 350$	cs-vcs
480	11.5	$1200 \pm 400$	cs-vcs
500	12.0	$1500 \pm 500$	vcs
520	12.4	$1700 \pm 600$	vcs-g
540	12.9	$2100 \pm 700$	vcs-g
560	13.4	$2300 \pm 800$	vcs-g
580	13.9	$2800 \pm 900$	vcs-g
600	14.3	$3000 \pm 900$	g
620	14.8	$3700 \pm 900$	g-p
640	15.3	$4000 \pm 1000$	g-p
660	15.8	$4500 \pm 1100$	g-p
680	16.3	$4800 \pm 1100$	g-p
700	16.7	$5100 \pm 1200$	g-p
720	17.2	$5600 \pm 1200$	p
740	17.7	$6200 \pm 1500$	p

\*Particle sizes determined for the range of volumetric specific heats discussed by *Edgett and Christensen* (1991, Figure 2).

### 5.5.3.1 Uncertainties

Caution is required in the interpretation of thermal inertia values because it is influenced by multiple factors. These include, among others, dust opacity, the presence of different grain sizes, the effects of pressure and topography, sub-surface layering, the influence of grain packing on bulk density, and water ice clouds to the extent they are not accounted for in the model [*Fenton and Bandfield*, 2003; *Ferguson et al.*, 2006a]. Thus, for example, pressure may affect the conversion from TI to particle sizes if the assumed average surface pressure is unrealistic for the location (because the specifications of the 'average' Martian surface pressure given in the literature are inconsistent, e.g. ~5 mbar [*Fenton and Mellon*, 2006; *Ferguson et al.*, 2006a], 5.6 mbar [*Kieffer et al.*, 1992a], 6.1 mbar [*Christensen et al.*, 1998], 7 mbar [*Haberle and Jakosky*, 1991]). However, this pressure effect is not very strong, and estimated grain sizes remain in the same range if pressure varies by about 1 mbar [*Presley and Christensen*, 1997b]. Moreover, exact individual pressure values measured by TES for every dune field in this study range from 5.6 to 6.1 mbar and thus do not vary by more than 1 mbar from the pressure value used by *Edgett and Christensen* (1994) for the conversion. Topography effects occur through daytime heating which, being more or less dependent on the orientation of the slopes, affects slope surface temperatures differently. This influence can be reduced by using night-time TI measurements [*Edgett and Christensen*, 1994]. Particle shape is another influencing factor because non-spherical grains have more grain-to-grain contact and thus a greater thermal conductivity [*Edgett and Christensen*, 1991]. Therefore, the lack of information on how layering, grain shape, and grain size mix affect thermal inertia restricts its interpretation as an indicator of particle size. An example of the influence of a hypothetical layer of dust covering a rock surface on surface temperature and thermal inertia is shown in Fig. 55. The different shapes and amplitudes of the temperature curves in Fig. 55a reflect variations in surface temperature responses caused by differences in the thickness of dust coatings. Thin dust covers have a minor effect on the temperature of a rock surface. The curves show a slighter thermal response resulting in just a minor increase in surface temperature around noon, when the diurnal temperatures reach their maximum. As the thickness of a dust cover increases, the rock surface adapts itself more and more to the thermal behaviour of dust: it shows a pronounced thermal response to temperature changes resulting in a higher temperature around noon. A 1-cm dust cover will completely mask the diurnal signature of rock (one diurnal skin depth of dust, cf. Sect. 5.5.1). Note that in comparison to the 0- $\mu\text{m}$  curve of pure rock, the maximum of the temperature curves representing a dust cover shifts to mid-day because of the faster thermal response of dust. Obviously, even a thin dust coating substantially affects the diurnal temperature signal of a rock surface because the dust insulates the rock from surface temperature cycles [*Mellon et al.*, 2008]. Fig. 55b shows the corresponding thermal inertia values around noon and midnight derived from these temperatures. This image again reflects the growing thermal response (and thus decrease in thermal inertia) with increasing dust cover thickness. Variations in the sinuosity of the day-time and night-time curves clearly show the notable day-time to night-time difference in thermal

inertia. Furthermore, they demonstrate the seasonal variability in apparent thermal inertia (see also *Mellon and Putzig, (2007); Putzig and Mellon, (2007b)*).

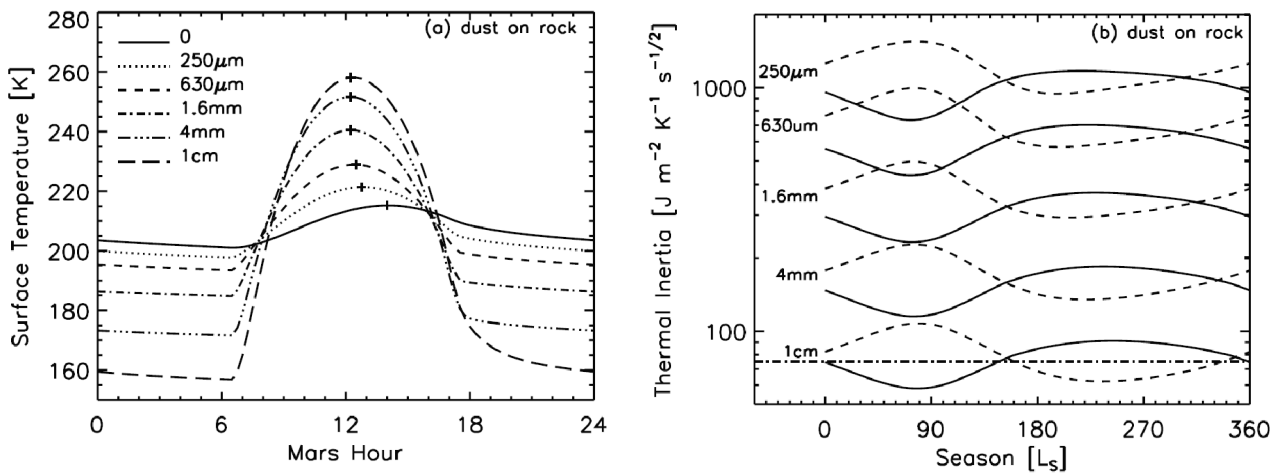


**Figure 55:** Varying diurnal temperature (a) and apparent seasonal thermal inertia (b) for a rock surface caused by a layer of dust representing different dust coating thicknesses [*Mellon et al., 2008*].

Layer thermal inertia values are assumed for rock =  $2250 \text{ J m}^{-2} \text{K}^{-1} \text{s}^{-1/2}$  and dust =  $75 \text{ J m}^{-2} \text{K}^{-1} \text{s}^{-1/2}$ . The horizontal dot-dashed line in (b) indicates component thermal inertia, i.e. the usual TI of dust. Night-time and day-time thermal inertia in (b) are shown as dashed and solid lines, respectively. Dust coating thicknesses are indicated (see text above for discussion and also *Mellon and Putzig (2007)*, *Putzig and Mellon (2007b)*, and *Mellon et al. (2008)*).

In sum, the larger the thermal inertia contrast between surface components (e.g. bedrock and dust), the larger the seasonal and diurnal effects [*Putzig and Mellon, 2007a; Mellon et al., 2008*]. A dust cover of only a few hundred micrometers thickness will influence the thermal signal. However, if it does not affect the albedo of the dune surface, it will not affect the thermal inertia value. Consequently, even if the presence of dust can be recognised in the spectrum of the dune surface it can be neglected in the interpretation unless it changes the albedo [*personal correspondence with N. Putzig*]. In other words: if the dust were thick enough to change the albedo, the dunes would not be distinctly darker. Consequently, if a dark dune is visible in an image, any existing dust cover is so thin as to remain below the observation wavelength, so that it has no influence on thermal inertia.

Because of the amount of data and localities, the thermal inertia analysis in this study had to be generalised in a way without, however, abandoning the objective of being as exact as possible. Therefore, single-point summer-time values over several years were measured and compared to each other for every locality. Extreme values that might have been caused by sensor inaccuracies or unusual dune covers (e.g. seasonal dust or ice), were excluded. The remaining measurements were averaged in order to obtain reliable values providing sufficient insight into the thermal behaviour of the dune fields. Moreover, most of the sand sheets were excluded from the thermal inertia interpretation because it could

not be ruled out that, due to insufficient thermal thickness, the TI values measured in these localities stemmed from the underlying surface.

To make sure that TI values are not influenced by latitude or elevation, they were plotted against the geographical parameters (Fig. 56). All values that do not correlate with latitude or elevation are due to the physical properties of the dunes, independent of the geographical position. The random distribution of the values shows that none of the correlations mentioned appears, confirming that the measured values reflect properties of the dune surfaces themselves. Only the highland-lowland distinction is recognizable by the prevalence of higher elevation values in southern latitudes and lower elevation values in higher latitudes. A similar test was conducted to rule out any dependency between the TI values and the mineralogy of the dark material. This is essential because one mineral type might exhibit coarser grain sizes or a generally higher density than another [Matthes, 2001]. If this influence were strong, it would result in TI values reflecting the thermal behaviour of the minerals and not the dune surface condition. Therefore, TI values were assigned to their respective mineralogy class and plotted against the latitudes of the localities (Fig. 57). The diagram shows no obvious correlation between mineralogy and thermal inertia values, as indicated by the random distribution. This confirms once more that the TI data measured can be interpreted as reflecting the dune surface condition. These non-dependencies are particularly important for the global analysis of an eventual correlation between dune surface condition and geographical location.

Although it is not possible to develop a characterization of physical properties from thermal inertia alone, it is helpful in estimating grain sizes and provides significant insight into the physical nature of surfaces [Ferguson *et al.*, 2006a]. Moreover, it is not necessary for this analysis to know the exact grain size of a dune field, but merely to divide the dunes into movable (sand-sized grains pointing to loose material) and immovable dunes (particle sizes greater than typical dune sand pointing to cemented grains or indurated surfaces, see Sect. 5.5.2 for a discussion). Therefore, the results of the thermal inertia analysis provide sufficient accuracy for use in this study.



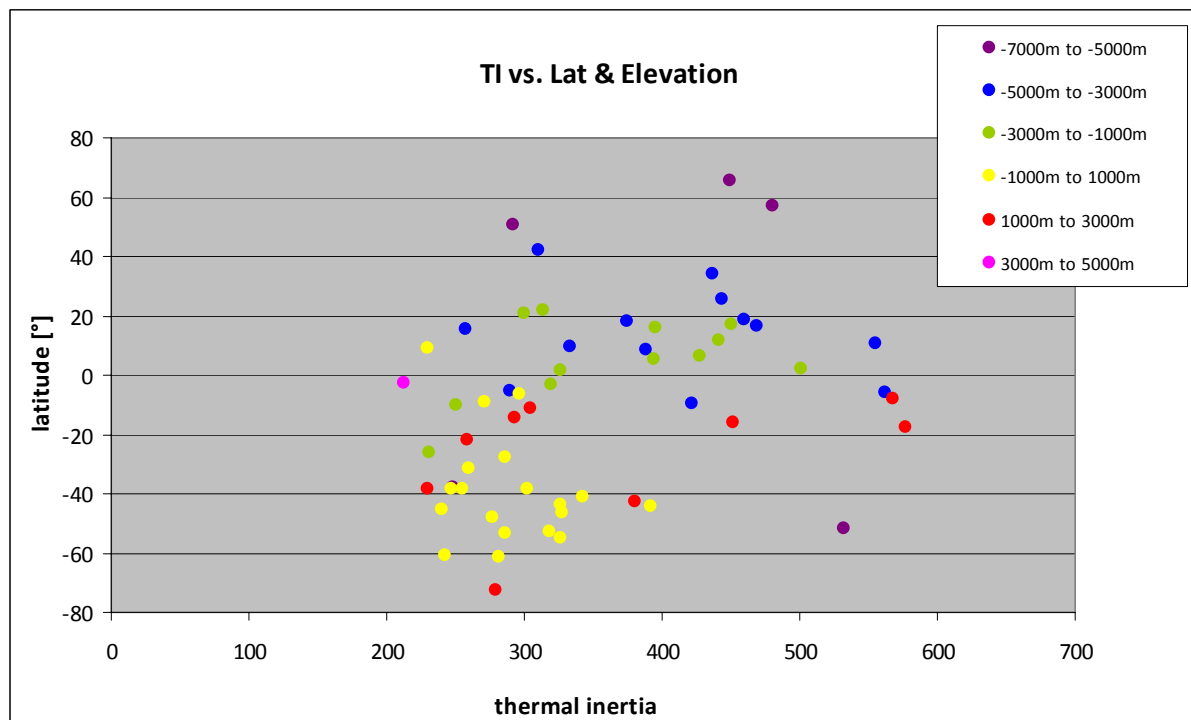


**Figure 56:** Thermal inertia versus latitude and elevation (TI is given in  $\text{J m}^{-2} \text{K}^{-1} \text{s}^{-1/2}$ ).

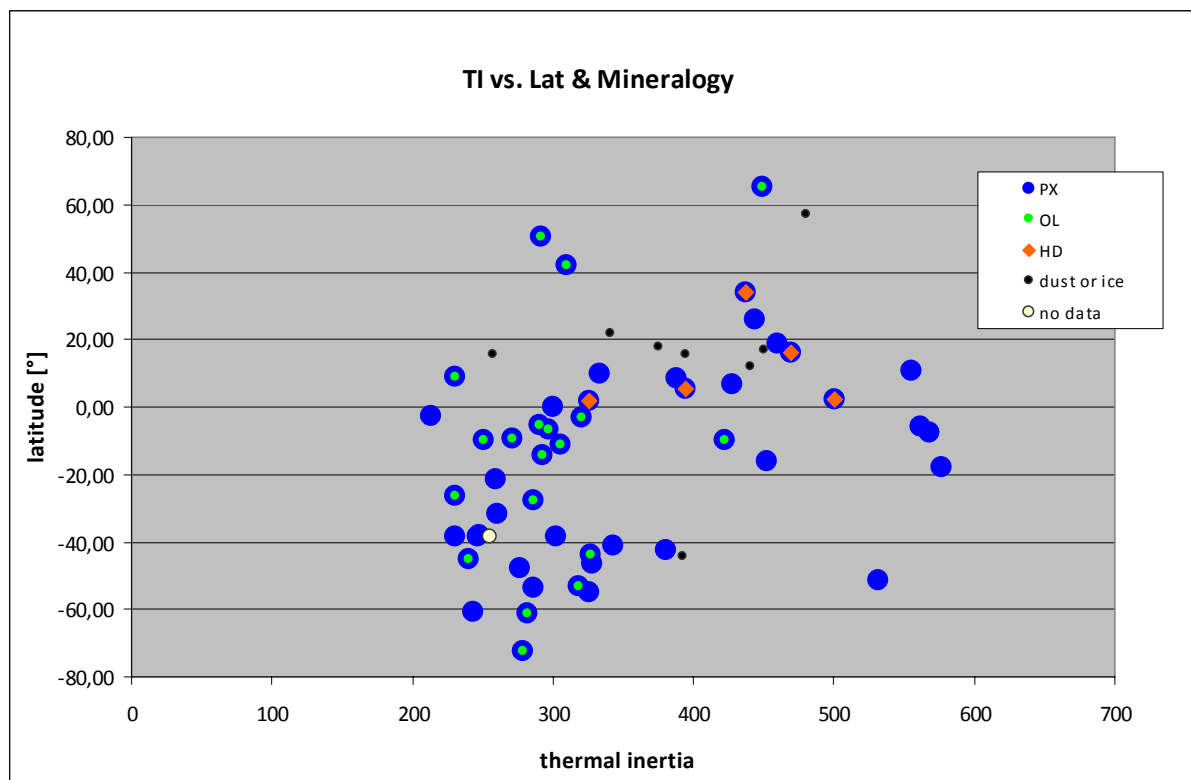


**Figure 57:** Thermal inertia versus latitude and mineralogy (TI is given in  $\text{J m}^{-2} \text{K}^{-1} \text{s}^{-1/2}$ ).

### 5.5.4 Results

TI data for every locality were derived by the method described in Sect. 4.4. A sharp boundary between TI values corresponding to unconsolidated surfaces of movable grains and TI values symbolizing consolidated surfaces or immovable material can not exactly be defined. According to *Edgett and Christensen* (1991), the average grain size of Martian dunes covers the medium to coarse particle size range. Consequently, grains of that size are movable on Mars and can be deposited as dunes (cf. Sect. 3.1 and *Edgett and Christensen* (1991)). This, in turn, implies that materials having greater particle sizes (very coarse sand or greater,  $\geq 900 \mu\text{m}$  [*Wentworth*, 1922]) are not movable by wind on Mars today. This assumption is confirmed by the diagram by *Greeley et al.* (1980) (Fig. 9 in Sect. 3.1). According to the findings of these authors, the aeolian transport of a particle with a size of  $800 \mu\text{m}$  would require wind speeds of about 210 m/s at an average Martian surface pressure of 5 mb and an average temperature of 195 K on a flat low-friction surface of erodable grains. Even on a surface with a higher friction (containing cobbles and boulders), the wind would need to reach velocities of approximately 70 m/s corresponding to friction speeds of  $\sim 4.3 \text{ m/s}$ . As discussed in Sect. 3.1 and 5.4 winds on Mars do not reach such high velocities. The diagram by *Edgett and Christensen* (1991) (Fig. 8 in Sect. 3.1) implies that for  $800 \mu\text{m}$ -sized grains a threshold friction speed of  $\sim 3.5 \text{ m/s}$  is required. Although these theoretical estimations vary slightly they are reasonable because even the highest reported wind speeds of 40 to 50 m/s reaching friction speeds of 2.2 - 4.0 m/s [*Moore*, 1985] could not transport very coarse-grained particles. Consequently, it has to be assumed that particle sizes of very coarse and above ( $\geq 900 \mu\text{m}$ ) cannot be moved on Mars.

Thus,  $900 \mu\text{m}$  is a feasible boundary between movable and immovable grains and is considered to correspond with the transition from unconsolidated to consolidated dune surfaces in this study. On a consolidated surface, the pore spaces between the grains are filled with dust or mobilised salts that act as cement, resulting in a surface that no longer consists of loose grains [*Jakosky and Christensen*, 1986; *Thomas et al.*, 2005]. See Sect. 5.7 for a discussion of such processes. Thus, the consolidation of smaller grains elevates the effective particle size to the higher ranges, resulting in a higher thermal conductivity and thus in a higher thermal inertia [*Jakosky and Christensen*, 1986] (cf. Sect. 4.4). As mentioned above, dunes that consist of medium to coarse-grained sand [*Edgett and Christensen*, 1991] should exhibit TI values corresponding to that particle size range. In turn, higher TI values of dunes (very coarse sand or higher) should not be interpreted as indicating greater grain sizes but as reflecting surface consolidation. Following Table 10 the boundary between coarse-grained to very coarse-grained sand lies at a particle size of 800 to  $900 \mu\text{m}$  and a thermal inertia of 400 to  $420 \text{ J m}^{-2} \text{ K}^{-1} \text{ s}^{-1/2}$ . For that reason, the boundary between unconsolidated, movable dunes and consolidated, immovable dunes was assumed to be around  $400 \text{ J m}^{-2} \text{ K}^{-1} \text{ s}^{-1/2}$ .

The results show that there are dunes whose intermediate TI values indicate sand-sized material as well as dunes that exhibit higher TI values, interpreted as indicating immovable material or duricrust. Fig. 58 gives examples of these two cases. The barchan dune field on a crater floor located at Tyrrhena Terra (Fig. 58a), shows thermal inertia values of 266 to 305  $\text{J m}^{-2} \text{K}^{-1} \text{s}^{-1/2}$  corresponding to fine sand and medium sand (see Table 10, [Edgett and Christensen, 1994]. Following the definitions by Fergason and Christensen (2003) and Fenton and Mellon (2006), these TI values correspond to medium to coarse-grained sand. All TI interpretations of these values point to loose movable material. Consequently, dune fields exhibiting such intermediate TI readings ( $< 400 \text{ J m}^{-2} \text{K}^{-1} \text{s}^{-1/2}$ ) are interpreted to have unconsolidated surfaces and might be active today. By contrast, the dune field in Reuyl Crater (Fig. 58b) exhibits TI values ranging from 409 to 465  $\text{J m}^{-2} \text{K}^{-1} \text{s}^{-1/2}$ , which correspond to very coarse sand ( $> 900 \mu\text{m}$ ) according to Table 10. Fergason and Christensen (2003) and Putzig *et al.* (2005) even interpret such TI values as indicating resistive outcrops or duricrust. Accordingly, dune fields exhibiting such high TI values ( $> 400 \text{ J m}^{-2} \text{K}^{-1} \text{s}^{-1/2}$ ) are assumed to have consolidated surfaces and might thus be inactive at the time of observation. The BTR analyses of these dune fields show analogous results, substantiating this interpretation.

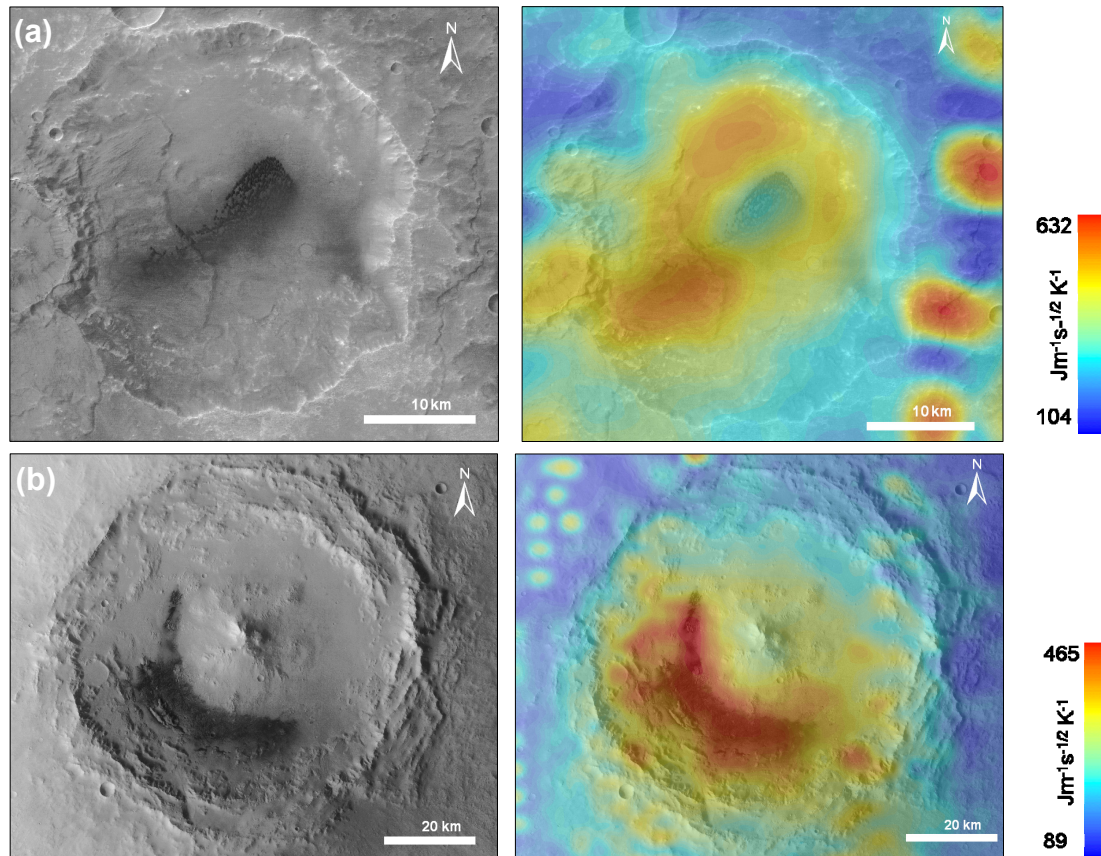


**Figure 58:** Comparison of low and high thermal inertia dunes.

(a) Barchan dune field in a crater in Tyrrhena Terra (14.3°S, 95.8°E), showing mean TI values around  $293 \text{ J m}^{-2} \text{K}^{-1} \text{s}^{-1/2}$  indicating unconsolidated sands (left: HRSC nadir 0038\_0000, right: gridded TES thermal inertia overlain onto HRSC, the high value spots on the right hand margin are artefacts of TES data processing). (b) Dune field in Reuyl Crater (9.7°S, 166.9°E) showing mean TI values around  $445 \text{ J m}^{-2} \text{K}^{-1} \text{s}^{-1/2}$  indicating a consolidated surface (left: HRSC nadir mosaic of 1945\_0000 and 1947\_0000, right: gridded TES thermal inertia overlain onto HRSC).

Analyses of huge dune fields, such as that of Kaiser Crater, show that a proportion of the dunes display high TI values indicating immovable material, whereas the bulk of the dune field shows the thermal behaviour of unconsolidated movable material (Fig. 59). This is reasonable for huge dune fields where unconsolidated and consolidated dunes may coexist. This conclusion is confirmed by high-resolution MOC images of these high-TI dunes that reveal gullies on the dune surfaces, which cannot develop on loose surfaces (see Fig. 71, Sect. 5.7). The spatial resolution of the TES data used in this work allows only predictions for entire dune fields, not for individual dunes. A detailed morphological and thermal analysis of every single locality using high-resolution image and thermal data would be necessary to arrive at reliable predictions for individual dunes in huge dune fields.

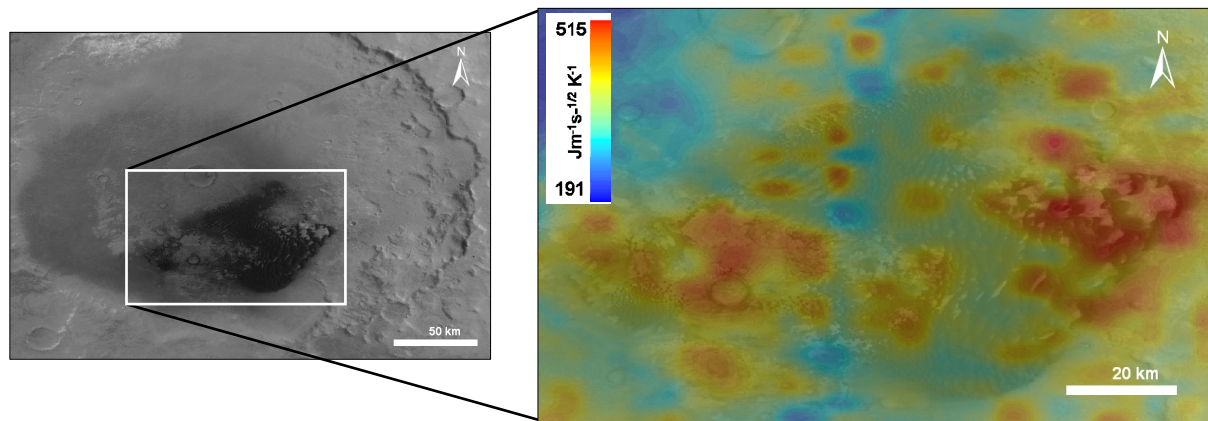


**Figure 59:** Results of thermal inertia analysis of Kaiser Crater dune field (46.5°S, 18.8°E).

**Left:** HRSC nadir image of Kaiser Crater (HRSC mosaic of 2148\_0000, 2159\_0001, 2181\_0001, and 2628\_0001). **Right:** Detail of Kaiser Crater dune field showing higher and lower TI values indicating movable and immovable dunes coexisting in the dune field (colour-coded TI TES overlaid on HRSC).

After the classification described above, results were incorporated and illustrated in the GIS, providing a global distribution of night-time warm/cold deposits (Fig. 62) and high/low thermal inertia measurements (Fig. 63). It is important to note that these images do not yet reflect the distribution of movable and immovable dark deposits on Mars. To obtain this, a combined interpretation of all results is needed. This will be presented in the next section.

The distribution of dark material deposits that are warmer/cooler than their surroundings at night-time (Fig. 62) show cooler dark material preferentially deposited in the highland regions and warm deposits in the lowland regions that is roughly aligned with the lowland/highland boundary. However, there is no correlation between warmer/cooler dunes and lower/higher elevations. The characteristic of temperature differences is governed by local conditions of dust opacity, crater floor material, and dune condition. As mentioned in Sect. 5.5.2, the BTR difference analysis can only give a first impression of the night-time thermal behaviour of a material and its ability to retain or lose heat at night. The results of this analysis will be incorporated in the combined analysis following in the next section.

The distribution of localities showing low and high TI values (Fig. 63) shows a slight correlation between low TI values and the southern highlands and between high TI



values and lower altitudes, similar to the result image of the BRT difference analysis. As the diagram in Fig. 56 shows, this distribution is not a geographical effect caused by higher/lower surface pressures at lower/higher elevations, respectively (lower surface pressures result in lower surface temperatures and thus in a lower apparent thermal inertia [*Mellon et al.*, 2000; *Mellon et al.*, 2008]) and can thus be assumed to be material immanent. However, these TI results do not allow concluding on material mobility yet, because the values measured cannot be interpreted as reflecting dark material properties in every case. For example, locations with thin sheets of dark material providing insufficient thermal thickness permit no conclusions regarding material properties, because the measured TI values are probably derived from the underlying crater floors. For example, the high TI values measured at the localities named 'Thaumasia 1' and 'Thaumasia 2' (Fig. 60) cannot be interpreted as immovable material because, due to the insufficient thermal thickness of the thin sand sheets, they are probably reflecting properties of the crater floor (see also Table 11).

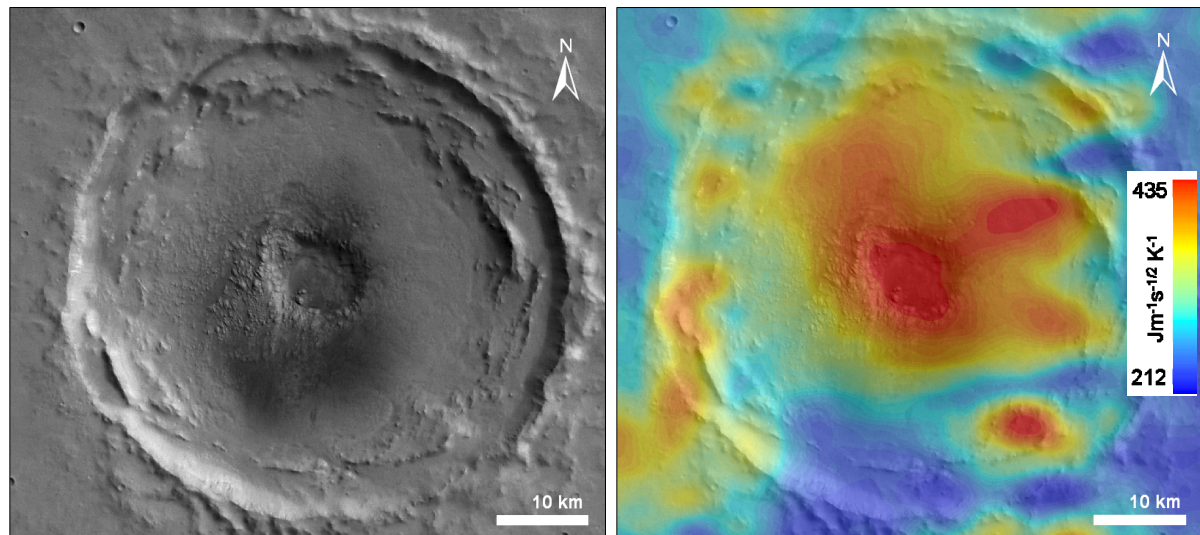


**Figure 60:** Thermally thin dark sand sheet in a crater in Thaumasia Planum (16.0°S, 296.3°E).

**Left:** HRSC nadir 0482\_0000. **Right:** TES TI overlaid on HRSC. The TI measurements do not correlate with the distribution of the dark sand sheet. The high TI values measured are probably derived from the solid crater floor and do not provide thermal information about the dark material.

The following diagram shows that the TI values for most of the dunes surfaces analyzed correspond to sands with grain sizes of up to 1200  $\mu\text{m}$ . It is obvious that thermal inertia correlates with grain size because grain size is calculated from TI. Note that the number of measurements is not equal to the number of localities analyzed because thermal inertia could not be determined at every location. Further statistics can be found in the database in the Appendix.

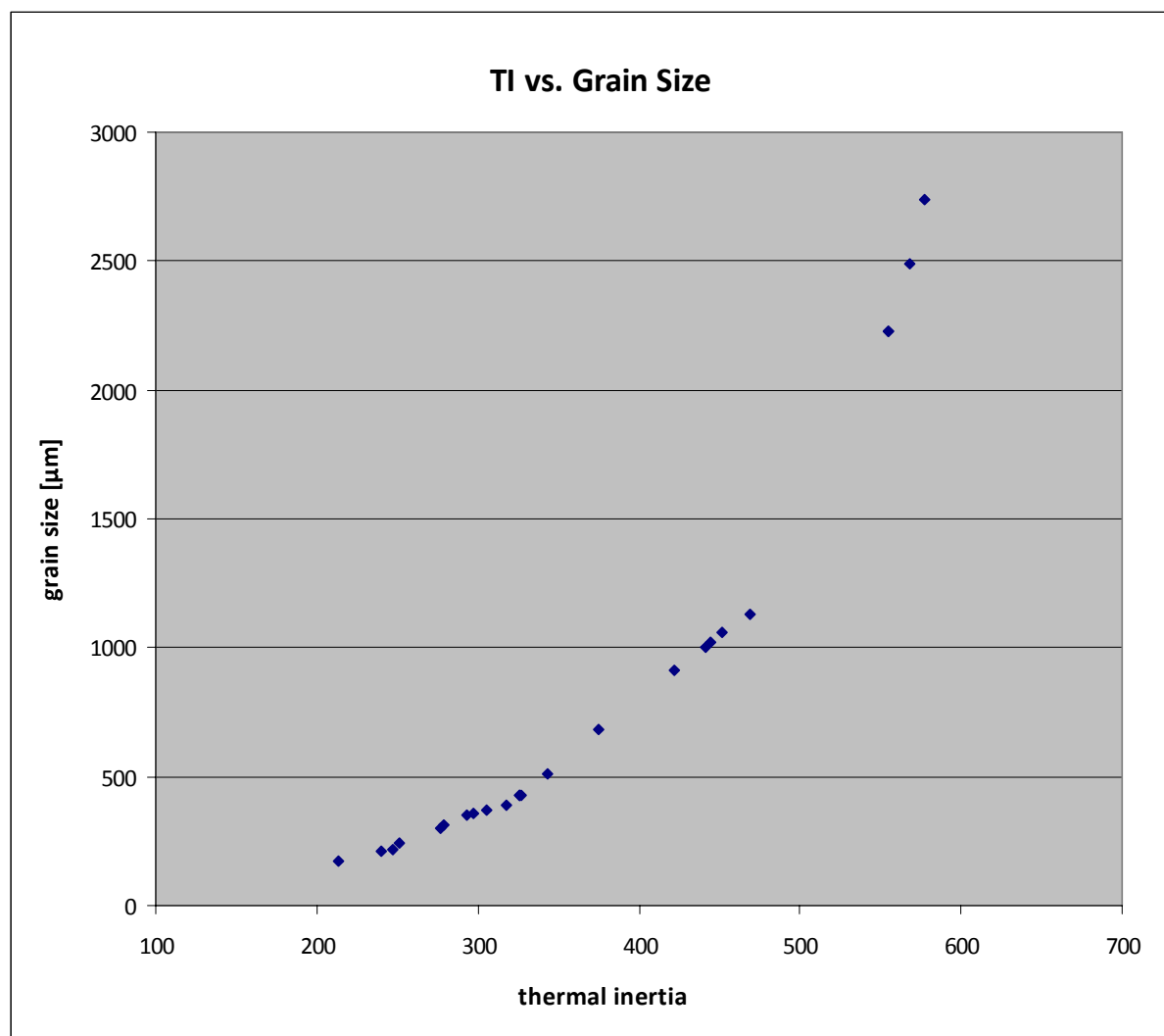


**Figure 61:** Thermal inertia versus grain size demonstrating the correlation of both parameters.

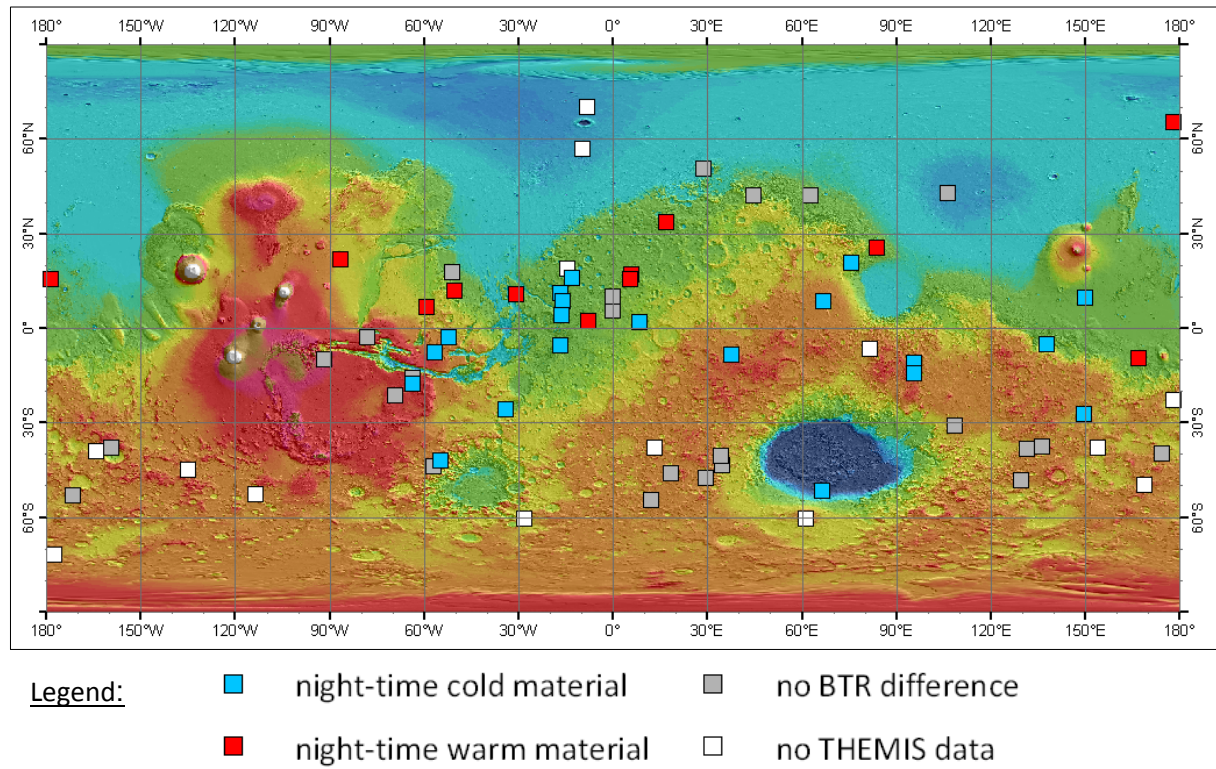


**Figure 62:** Global distribution of night-time warm and night-time cold dunes/sand sheets. (cf. Fig. 63 and 67, see text for discussion, background: MOLA topography map)

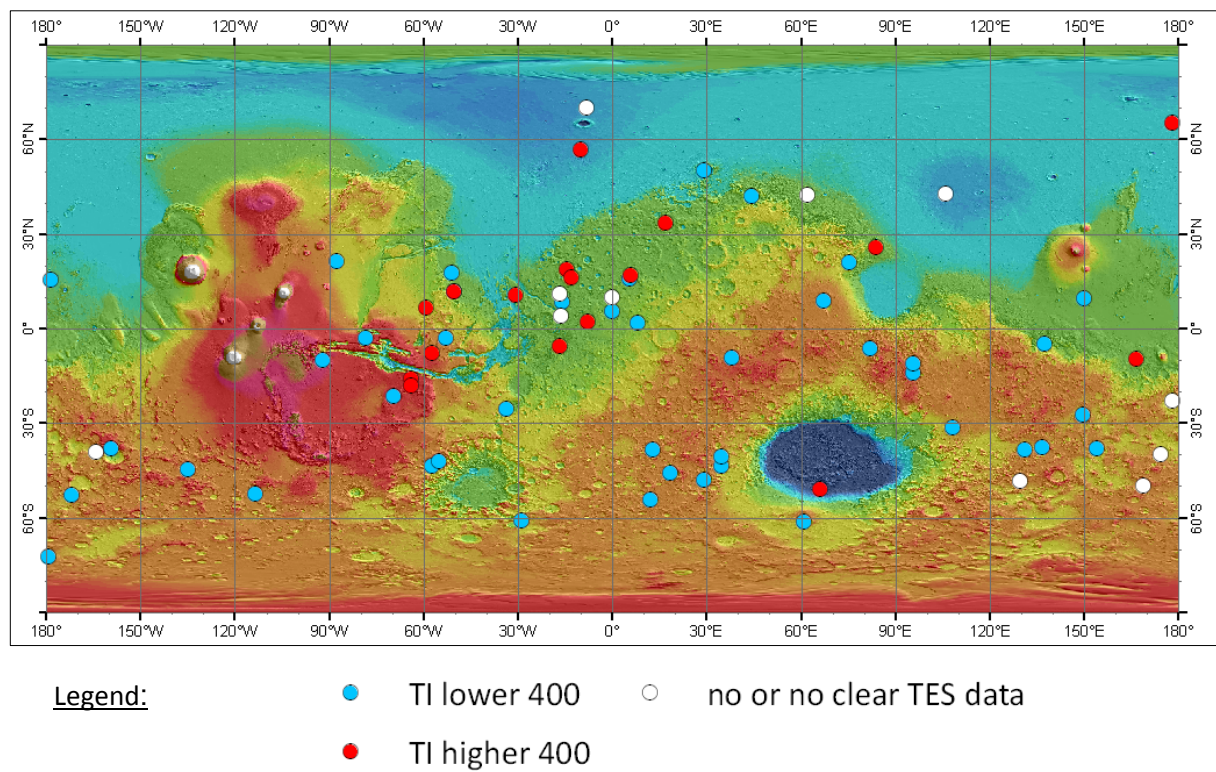


**Figure 63:** Global distribution of localities showing high and low night-time thermal inertia values. (TI is given in  $\text{J m}^{-2} \text{K}^{-1} \text{s}^{1/2}$ ; cf. Fig. 62 and 67, see text for discussion, background: MOLA topography map)